

Website publication 19 November 1998

NeuroReport 9, 3669–3674 (1998)

THE functional magnetic resonance (fMRI) technique can be robustly used to map functional activation of the visual pathway including the primary visual cortex (V1), the lateral geniculate nucleus (LGN), and other nuclei of humans during visual perception stimulation. One of the major controversies in visual neuroscience is whether lower-order visual areas involve the visual imagery process. This issue was examined using fMRI at high magnetic field. It was demonstrated for the first time that the LGN was activated during visual imagery process in the human brain together with V1 and other activation. There was a tight coupling of the activation between V1 and the LGN during visual imagery. *NeuroReport* 9: 3669–3674 © 1998 Lippincott Williams & Wilkins.

**Key words:** fMRI; Human brain; Lateral geniculate nucleus; Primary visual cortex; Pulvinar nucleus; Visual imagery

## Human primary visual cortex and lateral geniculate nucleus activation during visual imagery

Wei Chen,<sup>CA</sup> Toshinori Kato,  
Xiao-Hong Zhu, Seji Ogawa,<sup>1</sup>  
David W. Tank<sup>1</sup> and Kamil Ugurbil

Center for Magnetic Resonance Research,  
Department of Radiology, University of  
Minnesota, 385 East River Road, Minneapolis,  
MN 55455; <sup>1</sup>Bell Laboratories Innovations,  
Murray Hill, NJ 07974, USA

<sup>CA</sup>Corresponding Author

### Introduction

Visual mental imagery is the recreation of perceptual experiences using the 'mind's eye' in the absence of a retinal input. Whether this cognitive process is subserved by the same neural substrate as visual perception is one of the major controversies in visual neuroscience.<sup>1,2</sup> There is general agreement that several higher-order cortical areas in the parieto-occipital and temporo-occipital visual association pathways are involved in both visual perception and visual imagery process; however, the possible involvement of lower-order visual areas in visual imagery is intensely debated. Based on positron emission tomography (PET) data that failed to detect any activity in V1 and adjacent visual areas such as V2 and V3,<sup>3</sup> it has been argued that lower-order visual areas are predominantly computational and not representational and, as such, not obligatory in recreation of an already computed representation. In the opposing view, involvement of topographically organized visual areas is thought to be required in order to construct the geometry of shape during visual imagery; consequently, visual perception and imagery must share a common mechanism in V1 as well as in adjacent, retinotopically organized, lower-order visual areas.<sup>4,5</sup> It has also been proposed that attentional components in visual imagery process

may enhance activities in the pulvinar nucleus and subsequently in V1 through the reciprocal connections between the pulvinar and V1.<sup>6,7</sup> Irrespective of the specific mechanistic considerations, however, the present state of the debate at an experimental level involves the fundamental question of whether the primary visual areas are activated during visual mental imagery. Despite recent evidence from PET and functional magnetic resonance imaging (fMRI) studies showed V1 activation during visual imagery.<sup>4,8,9</sup> This debate persists, in part, because the primary visual cortex activation in the human brain has not been consistently observed during visual imagery task performances, possibly as a consequence of the detection insensitivity of the non-invasive methods employed, and/or the nature of the tasks utilized. Therefore, demonstrating that the primary visual cortex is indeed an integral component of visual mental imagery requires additional and clearly robust observations of activation in V1. Further evidence would also be provided by the observation that subcortical areas reciprocally connected with V1 are also activated.

The LGN is a primary target of retinal afferent and, in turn, it projects to V1.<sup>10</sup> A very strong back projection from V1 to the LGN is also present. Although to our knowledge the ratio of backward to forward projection fibers has not been determined in

the primate, in the cat the ratio is about 10:1.<sup>11,12</sup> If V1 is indeed involved in visual imagery, this strong back projection from V1 to the LGN might produce the LGN activation even in the absence of a visual perception stimulus. However, the functional mapping of the LGN activation has been unsuccessful for most existing neuroimaging techniques due to their limitations of detection sensitivity and/or spatial resolution, and the small size of the LGN.

The fMRI technique based on blood oxygenation level dependent (BOLD) effect provides a sensitive tool for mapping human brain function.<sup>13–15</sup> In addition, fMRI at high magnetic fields can further enhance the BOLD contrast, and increase detection sensitivity to microvasculature that translate into enhanced spatial specificity in functional brain mapping.<sup>16</sup> Recently, we demonstrated that the LGN activation in the human brain can be robustly detected during visual perception using fMRI at a high magnetic field (4 Tesla).<sup>17</sup> In this study, the same fMRI technique was used to examine if the V1 and the LGN activation were present together with activation in the higher-order visual areas during visual mental imagery process.

## Materials and Methods

**Subjects:** Fourteen healthy right-handed volunteers participated in these experiments (five males and nine females; mean age 28 years old; range 19–57). All participants were recruited from the academic environment of the University of Minnesota. This study was approved by the Institutional Review Board of the University of Minnesota Medical School.

**Experimental design:** Two visual imagery tasks were designed. In the ‘hometown walking’ visual imagery task, the participants were asked to imagine that they were walking in their hometowns that were most familiar to them, and were looking at objects within the scene, but not focusing on the walking component itself. This task is similar to the route finding task utilized by Roland *et al.*,<sup>3</sup> except that the participants were asked to ‘walk’ in their familiar hometowns, a task involving long-term memory storage, and they were not given a specific starting point or queried about their end point. In the ‘flashing light’ visual imagery task, the participants were asked to imagine the flashing light pattern of a goggle stimulator which they experienced before the beginning of the fMRI session. This task differed from the task used by LeBihan *et al.*,<sup>8</sup> in that the subjects performed the visual imagery task and the visual stimulation using a LED goggle in an interleaved way. In our study, the participants were

guided to watch and memorize the flashing light pattern of a LED goggle (GRASS Instrument, Quincy, MA, USA) flashing at 8 Hz before the experiment started; the flashing light imagery task was performed ~1 h later. All experiments were performed in a completely darkened room; during the visual imagery experiments, the participants were asked to keep their eyes closed at all times and to relax and refrain from generating any visual images during the control periods. Some subjects performed both visual imagery and visual perception tasks in the same session. The same LED goggle stimulator at 8 Hz was used for the visual perception experiments in comparison with the control periods in darkness.

**Image acquisition:** All fMRI experiments were performed on a Varian (Palo Alto, CA) console interfaced with a Siemens (Erlangen, Germany) 4 Tesla whole body system equipped with a head gradient coil insert. A quadrature head birdcage probe and quadrature surface coil were used for MRI signal excitation and observation. Subjects laid supine in the MRI scanner.

Conventional blipped echo-planar imaging (EPI) was used to acquire multislice images (gradient echo;  $T_2^*$ -weighted, and  $64 \times 64$  matrix size) during task and control periods for generating fMRI maps. Twenty to twenty-six contiguous axial images (6 mm slice thickness:  $24 \times 24$  cm<sup>2</sup> field of view (FOV)) covering the entire brain were obtained for four participants; 24–31 contiguous sagittal images (5 mm slice thickness,  $24 \times 24$  cm<sup>2</sup> FOV) were acquired for six participants, and 17–22 contiguous coronal images (5 mm slice thickness,  $20 \times 20$  cm<sup>2</sup> FOV) were acquired for four participants. The typical imaging acquisition parameters were 25–30 ms echo time, 50 ms/image and 3 s per multislice image set. Three control and two task periods were designed in an interleaved way. Twenty image sets were acquired in each of the five consecutive periods (1 min for each period and 5 min for each experiment). Additionally, multislice ( $128 \times 128$  pixels)  $T_1$ -weighted Turboflash images matching the same FOV, slice positions and orientations, as in functional images, and three-dimensional (3D) MDEFT image data set<sup>18</sup> were acquired for anatomy information. The multislice capability of fMRI and 3D anatomical image were used to generate 3D functional maps, so as to resolve the LGN from adjacent relevant structures (e.g. the pulvinar nucleus) and to visualize the LGN activation together with the V1 activation. A motion detector was used to monitor head movements during fMRI studies. If significant head movements were detected during fMRI acquisition, the experiment was terminated and

the data set was excluded from further data analysis, and the subject was asked to repeat the same experiment.

*Image processing and statistical analysis:* The acquired fMRI raw data was Gaussian filtered in the k-space for the signal-to-noise ratio (SRN) enhancement (full width at half maximal (FWHM) of the Gaussian kernel was 1.7 pixels). The filtered data were Fourier-transformed and analysed using functional imaging software STIMULATE developed in our laboratory. The fMRI maps were generated by comparison of  $T_2^*$ -weighted EPI images acquired between task and control periods using the period cross-correlation statistical methods based on the shape of the response in a pixel time course compared with the shape of a reference waveform as the decision criterion.<sup>19</sup> The reference waveform during the first 2–3 images (~6 s) acquired after the onset and cessation of each task period were specified as transition periods and modeled as linearly increasing (after the onset of visual stimulation) and linearly decreasing (after the termination of visual stimulation) over ~6 s to account for the finite response time of the hemodynamic changes. Activation pixels were determined by the following three criteria. (1) To eliminate false positives in areas of high signal fluctuation, pixels where the standard deviation of image to image MR signal fluctuation was > 2.0–3.0% relative to the mean MR signal during all control periods were excluded from the cross-correlation analysis. High standard deviation areas are usually found in large vessels,<sup>20</sup> on the edge of the brain and CSF space (due to edge effects and pulsatile flow of CSF) and in regions of poor SNR in EPI images (e.g. outside of the brain in EPI ghosts and in areas of poor homogeneity where significant signal loss has occurred inside of the brain). The criterion for setting the threshold for the standard deviation cut off was based on preserving most pixels inside the brain tissue and especially in the regions of interest (e.g., the LGN and V1 areas in this study). (2) Only pixels which correlated with the reference waveform with a cross-correlation coefficient (cc) above a threshold were included in fMRI maps. The minimal cc threshold used in the period cross-correlation analysis was 0.3. The probability value for false positives showing activated pixels was < 0.003.<sup>19</sup> The cc threshold for each data set was determined by the quality of activation maps with maximal activation in the regions of interest (e.g. the LGN and V1) and minimal false activation pixels in the white matter areas. (3) Pixels with < 2 contiguous activated pixels were excluded from fMRI maps. This threshold of two pixel cluster size improves the effective statistical significance of the detected activation.<sup>21</sup>

The percentages of BOLD changes in the LGN were calculated by the comparison of the average signals between control and task periods. The number of the activated pixels in the LGN were taken from the slices of the fMRI maps showing maximal LGN activation.

The activated pixels were overlaid on the 3D  $T_1$ -weighted MDEFT image to generate a 3D fMRI map that could be resliced in any orientation to evaluate activation sites within the brain. The activated pixels were interpolated to match the matrix size of the 3D  $T_1$ -weighted MDEFT image.

## Results

Figure 1 illustrates a 3D view of a participant's brain displaying activation during the hometown walking visual imagery task. In this 3D view, activation can be seen on the cortical surface that can be visualized from the chosen view angle (Fig. 1a), and in V1 near the anterior calcarine fissure (Fig. 1b). Activation in parietal, temporal, frontal cortices and other areas were detected during the visual imagery tasks, and these areas can be seen in the 3D images displayed in Fig. 1. These results, however, are beyond the scope of this paper and are not discussed further.

Figure 2 illustrates the comparisons of fMRI maps between visual perception and visual imagery tasks performed in the same experimental session from the same participant shown in Fig. 1, the coronal images in this figure were extracted from the 3D data set by reslicing. Figure 2a shows the V1 and bilateral LGN activation during photic stimulation task. The LGNs in the two hemispheres were easily identified by their position related to the optic tract, their location superior to the hippocampal formation in the coronal view (Fig. 2a), and their proximity to the pulvinar and medial geniculate nucleus as discerned in the 3D images of the brain. The optic tract is seen clearly in both hemispheres near the optic chiasm, anterior to the mid-brain; proceeding posteriorly from the optic chiasm, it appears to merge with the mid-brain, and is no longer visualized with clarity as it runs along the cerebral peduncle. Following this curved tract (pointed to by the yellow arrows in the axial images of Fig. 2) should lead directly to the LGN, which is where the activated loci is identified as the LGN. The pulvinar nucleus in the thalamus, especially the inferior and adjacent lateral parts, were also activated bilaterally during most photic stimulation and visual imagery studies. The activated pulvinar regions are very close to the LGN neuroanatomically;<sup>22,23</sup> however, they were well resolved in the 3D reconstructed fMRI maps.<sup>17</sup> Primate studies suggest that the pulvinar nucleus is an integral part of the extrageniculate visual pathway.<sup>24</sup>

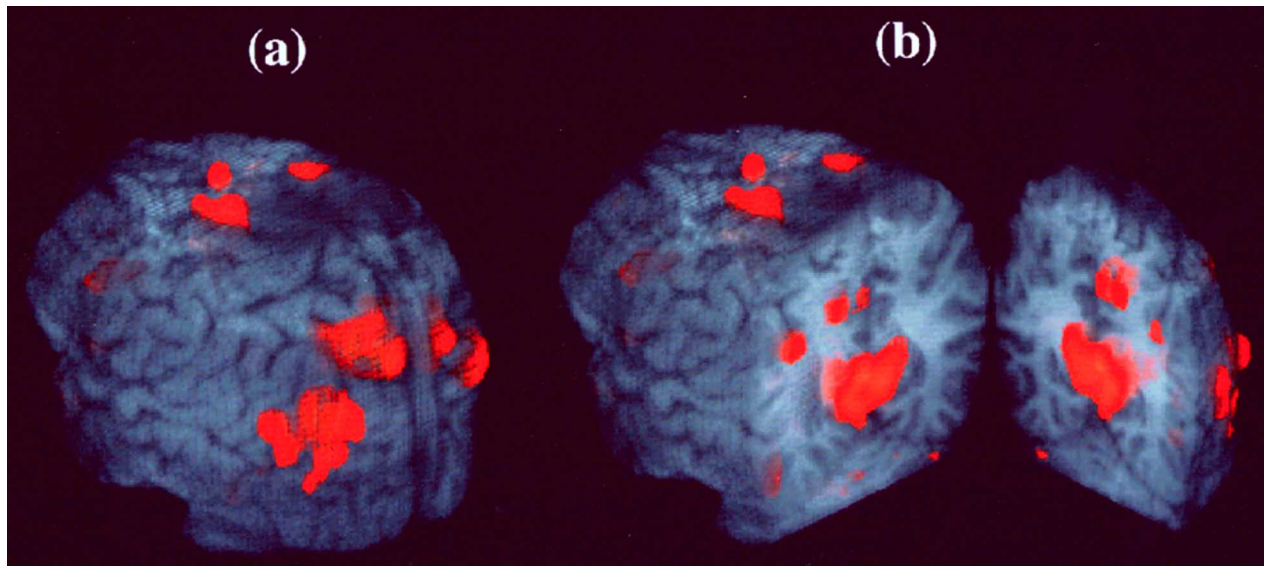


FIG. 1. Three-dimensional functional map obtained with 4 Tesla fMRI from a single participant during the hometown walking visual imagery task. Anatomical and functional data are presented in gray scale and color, respectively. The anatomical image was rendered sufficiently translucent so as to see the activation through the cortical surface that is in the sulci close to the surface. Activation present in more deeper structures or the surface of the brain 'hidden' from view is not visible in (a). (b) The image was 'sliced open', exposing the activation in the primary visual cortex near the calcarine fissure.

Our results indicate that the pulvinar nucleus involves the visual imagery process in humans.

Table 1 summarizes the results showing the number of participants who displayed activation in V1, the LGN, and the pulvinar nucleus and the averaged BOLD signal intensity change in the LGN.

The fMRI maps in Fig. 2b illustrate the activation in the LGN and V1 during the flashing light imagery task from an individual participant. The activation location in the LGN was the same as those observed during photic stimulation (Fig. 2a), but the activation size was relatively small. The V1 activation located the medial portion of the calcarine fissure. Twelve participants performed the flashing light visual imagery task. Five participants showed activation in both V1 and the LGN bilaterally and two participants displayed activation only in V1, but not in the LGN. All participants that had activation in V1 (7/7) displayed activation in the pulvinar nucleus as shown in Table 1. The averaged BOLD signal change in the LGN was  $1.1 \pm 0.3\%$  (range 0.60–1.96%). This value is similar to the value observed from photic visual stimulation.<sup>17</sup> The averaged two-dimensional pixel number of the LGN activation was  $3.9 \pm 1.1$  (range 2–6). Other participants (five subjects) failed to show activation in both V1 and the LGN, possibly due to difficulty in recalling and imaging the flashing light pattern, which they had encountered briefly before the study.

In the hometown walking imagery task, which involved long-term storage, all nine participants displayed robust activation in V1 and in the pulvinar

nucleus; eight showed activation in the LGN (five bilaterally and three unilaterally) as well as in V1 (Table 1; Fig. 2c). The locations of the LGN activation were consistent with that showing in the photic stimulation and the flashing light visual imagery task (Fig. 2a,b). The activated areas in V1 were shifted to the anterior portion of the calcarine fissure as illustrated in the axial and coronal fMRI maps in Fig. 2c and Fig. 1b. The averaged BOLD signal change in the LGN was  $0.8 \pm 0.3\%$  (range 0.46–1.30%). This is slightly less than the 1.1% observed from the previous study of photic visual stimulation.<sup>17</sup> The averaged two-dimensional pixel number of the LGN activation was  $3.3 \pm 0.7$  (range 2–4). This size ( $6.8 \times 6.8 \text{ mm}^2$  after ignoring the broadness by the Gaussian filter) is consistent with the expected LGN size in the human brain.

## Discussion

Our results demonstrate that the LGN as well as V1 are activated during visual mental imagery, with the activity in these two regions being tightly correlated. The success rate showing the LGN and V1 activation during the hometown walking imagery task was much greater than that during the flashing light imagery task (Table 1). It is speculated that the task difficulty and subject's performance may cause this difference, and it is relatively easier for subjects to imagine their familiar hometown than to imagine the flashing light. Therefore, the learning of the similar visual patterns through visual perception just before

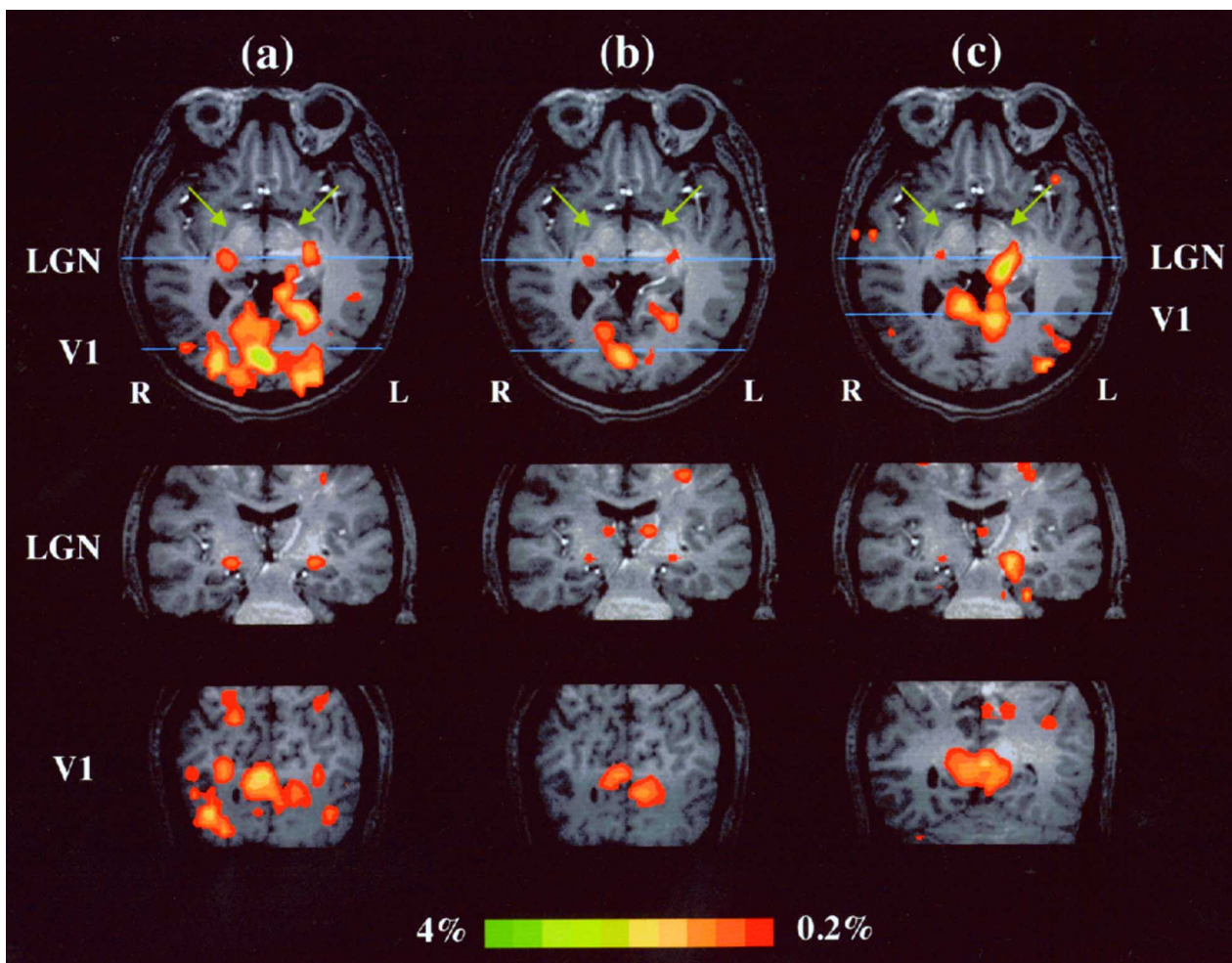


FIG. 2. Functional MRI maps of activation (in color) superimposed on anatomical images (gray scale) from a single individual during (a) the photic stimulation task; (b) flashing light visual imagery task and (c) hometown walking visual imagery task performed in the same experimental session. The maps in the top row illustrate the activation in the LGN and V1 areas in the axial orientation; the horizontal lines labeled the LGN and V1 represent the positions of the two coronal slices presented in the lower two rows; the yellow arrows in the axial images point to the curved optic tracts that lead directly to the LGN. The LGN activation on the left hemisphere (top row in c) during the hometown walking visual imagery task is partially overlaid with the activation in the pulvinar and hippocampus. Other activation was also shown in the thalamus during visual imagery tasks as shown in the medial row in (b) and (c). The coronal slice maps in the medial row show the activation in Brodmann area 6. The fMRI maps of visual perception as shown in (a) have been published by Chen *et al.*<sup>17</sup> and they are used here for comparing the anatomical locations of the LGN and V1 activation between visual perception and visual imagery tasks.

visual imagery studies may increase the activation in V1 and the LGN during the flashing light visual imagery task. This issue was examined recently using the same fMRI acquisition and paradigm described in this paper except adding a real visual perception experiment (flashing light) between the flashing light visual imagery experiments. Our preliminary results (not presented herein) demonstrate a significant increase of the V1 activation during visual imagery experiments after performing and learning visual perception. This indicates that not only the detection sensitivity of neuroimaging technique but also the subject performance of visual imagery task can affect the detection ability for functional mapping of the LGN and V1. This may partially explain the

controversial results in literature regarding whether the neurons in the V1 areas involve visual imagery.<sup>3,4</sup>

The comparison of the results between the two visual imagery tasks indicate that the location of the V1 activation may depend upon the content size imagined by subjects. The large imagery size during the hometown walking visual task activated the anterior portion in V1, whereas the relatively small imagery size during the flashing light visual imagery task activated the medial portion in V1. These observations were consistent with the results from PET studies using different mental imagery paradigms showing that large imagery images only activated the anterior V1, whereas, small imagery images activated the posterior V1.<sup>4</sup>

**Table 1.** Percentage of participants that displayed activation V1, the LGN, and the pulvinar nucleus in the thalamus during visual imagery tasks.

	Visual imagery of hometown walking (n = 9)	Visual imagery of flashing lights (n = 12) <sup>a</sup>	Visual imagery of flashing lights (n = 7) <sup>b</sup>
V1	100	58	100
Pulvinar	100	–	100
LGN	89	42	71
BOLD change in LGN <sup>c</sup>	0.8 ± 0.3	–	1.1 ± 0.3

<sup>a</sup>Only seven of the 12 subjects showed activation in V1.

<sup>b</sup>Data only from the seven subjects who showed activation in V1.

<sup>c</sup>Percentage signal intensity changes averaged from the participants who displayed LGN activation (mean ± s.d.).

The simplest explanation for our results is that activation of the LGN is through transmission conveyed to it from the strong back-projection known to exist from V1 to the LGN. This pathway is primarily produced by the axons of layer VI pyramidal cells in V1 suggesting that these neurons show increased firing rates during visual imagery. This activity may serve to regulate the visual input to V1 at the level of the LGN during visual mental imagery. The LGN may also receive input from the brain stem reticular formation,<sup>25</sup> and these connections may, in part, be responsible for the activation detected in the LGN as part of increased visual arousal during visual imagery tasks, with subsequent projection into V1 through the ascending connections between the LGN to V1. This mechanism can account for the contribution of the LGN and V1 activation during visual imagery, however, it cannot be exclusively responsible for the observed effects, since V1 activation detected would have been non-specific with the visual imagery task. However, activity seen in V1 during visual imagery was well localized to subregions of the primary visual cortex and was not the same for the two visual imagery tasks.

## Conclusion

Our results show, for the first time, that the LGN was activated during the visual imagery process in the

human brain together with V1 and pulvinar activation. There was a tight coupling of activation between the LGN and V1 during visual imagery. The possibility of detecting the LGN and V1 activation during visual imagery may depend on the task performance. The LGN and V1 activation during visual imagery may involve both visual arousal and visual representation. However, the distinction between these two components requires further studies. Finally, these results demonstrate that the fMRI technique is very useful for mapping brain function, including both small thalamic nuclei such as the LGN and the pulvinar nucleus and cortical areas during higher cognitive studies.

## References

- Roland PE and Gulyas B. *Trends Neurosci* **17**, 281–287 (1994).
- Kosslyn SM and Ochsner KN. *Trends Neurosci* **17**, 290–292 (1994).
- Roland PE and Gulyas B. *Cerebr Cortex* **5**, 79–93 (1995).
- Kosslyn SM, Thompson WL, Kim IJ and Alpert NM. *Nature* **378**, 496–498 (1995).
- Ishai A and Sagi D. *Science* **268**, 1772–1774 (1995).
- Sakai K and Miyashita Y. *Trends Neurosci* **17**, 287–289 (1994).
- Olshausen BA, Anderson CH and van Essen DC. *J Neurosci* **13**, 4700–4719 (1993).
- Le Bihan D, Turner R, Zeffiro TA et al. *Proc Natl Acad Sci* **90**, 11802–11805 (1993).
- Ugurbil K, Ogawa S, Menon R et al. Mapping brain function non-invasively by nuclear magnetic resonance. In: Sugushita M, ed. *New Horizons in Neuropsychology*, Amsterdam: Elsevier, 1994: 3–22.
- Hubel DH and Wiesel TN. *J Comp Neurol* **146**, 421–450 (1972).
- Murphy PC and Sillito AM. *J Neurosci* **16**, 1180–1192 (1996).
- Douglas RJ, Koch C, Mahowald M et al. *Science* **269**, 981–985 (1995).
- Ogawa S, Tank DW, Menon R et al. *Proc Natl Acad Sci USA* **89**, 5951–5955 (1992).
- Kwong KK, Belliveau JW, Chesler DA et al. *Proc Natl Acad Sci USA* **89**, 5675–5679 (1992).
- Bandettini PA, Wong EC, Hinks RS et al. *Magn Reson Med* **25**, 390–397 (1992).
- Menon RS, Kim SG, Hu X et al. Functional MR imaging using the BOLD approach: field strength and sequence issues. In: D. Le Bihan, ed. *Diffusion and Perfusion Magnetic Resonance Imaging*. New York: Raven Press, 1994: 327–334.
- Chen W, Kato T, Zhu XH et al. *Magn Reson Med* **39**, 89–96 (1998).
- Lee J-H, Menon R, Andersen P et al. *Magn Reson Med* **34**, 308–312 (1995).
- Bandettini PA, Jesmanowicz A, Wong EC and Hyde JS. *Magn Reson Med* **30**, 161–173 (1993).
- Kim S-G, Hendrich K, Hu X et al. *NMR Biomed* **7**, 69–74 (1994).
- Forman SD, Cohen JD, Fitzgerald M et al. *Magn Reson Med* **33**, 636–647 (1995).
- Robinson DL and Petersen SE. *Trends Neurosci* **15**, 127–132 (1992).
- Bender DB. *J Neurophysiology* **46**, 672–693 (1981).
- Rezak M and Benevento LA. *Brain Res* **167**, 19–40 (1979).
- Smith Y, Pare D, Deschenes M et al. *Exp Brain Res* **70**, 166–180 (1988).

ACKNOWLEDGEMENTS: The authors thank Dr S.G. Kim for stimulating discussion and technical assistance and Drs X. Hu, J. Strupp, P. Andersen and G. Adriano for software and hardware supports. This research was supported by P41 RR08079, a National Research Resource (NIH) grant.

Received 21 July 1998;  
accepted 7 September 1998